

# Charge and orbital excitations in $\text{Li}_2\text{CuO}_2$

Young-June Kim and J. P. Hill

*Department of Physics, Brookhaven National Laboratory, Upton, New York 11973*

F. C. Chou

*Center for Materials Science and Engineering, Massachusetts Institute of Technology, Cambridge, Massachusetts 02139*

D. Casa, T. Gog, and C. T. Venkataraman

*CMC-CAT, Advanced Photon Source, Argonne National Laboratory, Argonne, Illinois 60439*

(Dated: July 23, 2018)

We report a resonant inelastic x-ray scattering study of electronic excitations in  $\text{Li}_2\text{CuO}_2$ , an insulating compound comprised of ribbons of edge-sharing copper-oxygen chains. Three excitations, which show little dependence on momentum transfer, are observed in our measurements. The lowest energy excitation at  $\sim 2.1$  eV is dispersionless and is attributed to a localized  $d-d$  orbital excitation. We also observe two excitations at  $\sim 5.4$  eV and  $\sim 7.6$  eV which we assign to charge-transfer excitations. These high-energy excitations are also dispersionless along the copper-oxygen chain direction. However, in each case we observe a small energy dispersion along the direction perpendicular to the copper-oxygen ribbons, suggesting a significant interchain coupling in this system. We also discuss the possible implications of ferromagnetic nearest-neighbor intrachain coupling on the charge excitation spectra.

PACS numbers: 74.25.Jb, 71.70.Ch, 71.27.+a, 78.70.Dm

## I. INTRODUCTION

The magnetic properties of insulating copper oxide compounds have been drawn much attention over the past decade. Such systems include quasi-one-dimensional (1D) spin chains ( $\text{Sr}_2\text{CuO}_3$ ,  $\text{SrCuO}_2$ ,  $\text{CuGeO}_3$ ), spin ladders ( $\text{SrCu}_2\text{O}_3$ ,  $\text{Sr}_{14}\text{Cu}_{24}\text{O}_{41}$ ), and quasi-two-dimensional (2D) parent compounds of high temperature superconductors ( $\text{La}_2\text{CuO}_4$ ,  $\text{Sr}_2\text{CuO}_2\text{Cl}_2$ ). Many of these systems can be modeled by a simple Heisenberg spin Hamiltonian with only one parameter, that is, the superexchange coupling between copper spins,  $J$ . Unfortunately, calculating  $J$  is a difficult task, due to the strong electron correlations in these so-called Mott insulators. Part of the difficulty also lies in the fact that there is limited information on the electronic structure of these copper oxide compounds. Thus, spectroscopic studies of the electronic structure and excitations can provide important information leading towards an improved microscopic understanding of magnetism in insulating copper oxides.

$\text{Li}_2\text{CuO}_2$  has been frequently modeled as an edge-sharing chain compound,<sup>1,2,3,4,5,6,7</sup> that is, the copper-oxygen plaquettes in this material are connected by their edges with the Cu-O-Cu bond angle ( $\theta$ ) close to  $90^\circ$ . Electronic properties of  $\text{Li}_2\text{CuO}_2$  have been studied with optical conductivity,<sup>4</sup> x-ray absorption spectroscopy (XAS),<sup>6</sup> and electron energy-loss spectroscopy (EELS).<sup>7</sup> The consensus from these experiments is that  $\text{Li}_2\text{CuO}_2$  is a charge-transfer (CT) insulator, with a CT gap of  $2.2 \sim 2.7$  eV. This is in agreement with spin-polarized local density approximation (LDA) calculations by Weht and Pickett,<sup>8</sup> which found a gap of 2.5 eV. Another important observation is that there exist several

exchange paths between the copper spins and that none of these exchange interactions dominate, and as a result  $\text{Li}_2\text{CuO}_2$  cannot be described as a simple Heisenberg spin chain.<sup>6,7</sup> This intricate nature of the magnetic interactions is most clearly demonstrated by the magnetic phase transitions: Experimentally, the paramagnetic susceptibility of  $\text{Li}_2\text{CuO}_2$  exhibits an antiferromagnetic Curie-Weiss behavior, with a transition temperature  $T_N \approx 9$  K. However, the magnetic structure is composed of ferromagnetic chains, which are coupled antiferromagnetically. In addition, a second transition to canted ferromagnetic phase at  $\approx 2.8$  K has been observed by magnetization<sup>9</sup> and muon-spin rotation studies.<sup>10</sup>

Due to this complexity of the underlying spin Hamiltonian, it is difficult to experimentally determine the magnetic interactions in this system. Even the sign of  $J$ , that is, whether the nearest-neighbor coupling along the chain is ferromagnetic or antiferromagnetic is controversial. According to the Goodenough-Kanamori-Anderson rules,  $J$  is expected to be small, unlike the large antiferromagnetic superexchange coupling present in the case of a  $\theta = 180^\circ$  bond. In fact, calculations of Mizuno and coworkers<sup>4</sup> show that  $J$  is very sensitive to  $\theta$  for  $\theta$  close to  $90^\circ$ . In the case of  $\text{La}_6\text{Ca}_8\text{Cu}_{24}\text{O}_{41}$ ,  $\theta = 91^\circ$  and  $J$  is ferromagnetic ( $J < 0$ ), while for  $\theta = 99^\circ$  in  $\text{CuGeO}_3$ ,  $J > 0$ . For  $\text{Li}_2\text{CuO}_2$ , a powder x-ray diffraction study found  $\theta = 94^\circ$ .<sup>1</sup> A number of theoretical studies<sup>4,11,12</sup> suggest a ferromagnetic coupling between nearest-neighbor copper spins, which is consistent with the magnetic structure determined by powder neutron diffraction.<sup>2</sup> On the other hand, Boehm et al.<sup>5</sup> found that  $J$  is antiferromagnetic from their inelastic neutron scattering experiment. Clearly, further investigation of the electron hopping and the exchange interactions in this system is needed to de-

termine the spin Hamiltonian and elucidate the magnetic phase behavior.

In the present work, we have carried out resonant inelastic x-ray scattering (RIXS) experiments to study the electronic excitations of  $\text{Li}_2\text{CuO}_2$ . This technique allows one to probe the energy and momentum dependence of charge neutral electronic excitations, in particular focusing on those that involve the copper orbitals.<sup>13,14,15,16</sup> We have observed two types of excitations; one at 2.1 eV which we attribute to a localized  $d-d$  type orbital excitation, and excitations at 5.4 eV and 7.6 eV which we believe arise from CT-type processes in the Cu-O plaquettes. A small, but finite, dispersion of the latter along the direction perpendicular to the chain direction suggests that the interchain coupling is non-zero, supporting the conclusions of previous studies of magnetic interactions.<sup>5,6,11,12</sup> In addition, we compare our results with those of  $\text{CuGeO}_3$  and discuss the possible implications of ferromagnetic  $J$  on our RIXS spectra.

In the next section, we describe the experimental configurations used in the measurements. The incident energy dependence and the momentum dependence of the observed RIXS spectra are discussed in Sec. III A and Sec. III B, respectively. Finally, we will discuss the possible implications of the experimental results in Sec. IV.

## II. EXPERIMENTAL DETAILS

The experiments were carried out at the Advanced Photon Source on the undulator beamline 9ID-B. A double-bounce Si(333) monochromator and a spherical, diced, Ge(733) analyzer was used to obtain an overall energy resolution of 0.4 eV (FWHM). The scattering plane was vertical and the polarization of the incident x-ray was kept close to the  $\mathbf{c}$ -direction for the data reported here. Note that the edge-sharing  $\text{CuO}_4$  chain runs along the crystallographic  $\mathbf{b}$ -direction, and the Cu-O plaquettes lie perpendicular to the  $\mathbf{a}$ -direction.<sup>1</sup> A single crystal sample of  $\text{Li}_2\text{CuO}_2$  ( $a = 3.662$  Å,  $b = 2.863$  Å, and  $c = 9.393$  Å) was grown using the traveling solvent floating zone method. The crystal was cleaved along the (1 0 1) plane and mounted on an aluminum sample holder at room temperature. Since  $\text{Li}_2\text{CuO}_2$  is hygroscopic, care was taken to cleave the sample immediately before the experiment. It was then kept in vacuum throughout the experiment.

## III. EXPERIMENTAL RESULTS

### A. Incident Energy Dependence

In Fig. 1, we plot the incident energy ( $E_i$ ) dependence of the scattered intensity as a function of energy transfer ( $\omega$ ) at a fixed momentum transfer of  $\mathbf{Q}=(2.5 \ 0.1 \ 2.5)$ . Since (2.5 0.1 2.5) is near the Brillouin zone boundary, the elastic scattering intensity (i.e., at  $\omega = 0$ ) is not very

large. Three resonant features are observed in Fig. 1. The strongest feature has an excitation energy of  $\sim 5.4$  eV, and shows a large resonant enhancement in the intensity as the incident energy is varied through  $E_i \approx 9000$  eV, becoming weaker as the incident energy is tuned away from the resonance. A second feature at  $\sim 7.6$  eV shows slightly different resonance behavior. In addition, a third feature at 2.1 eV is very weak compared to the other two features, and resonates at much lower incident energy, around  $E_i \lesssim 8990$  eV. Note, because of geometrical constraints associated with the near backscattering angle of the Ge(733) analyzer crystal at these low incident energies, it was not possible to scan the incident energy below  $E_i = 8979$  eV.

To illustrate the resonance profile of these peaks, we plot in Fig. 2(a) the scattered intensity as a function of  $E_i$ , with the energy transfer fixed at these excitation energies. That is, the intensity as measured at the positions indicated by vertical dotted lines in Fig. 1 is plotted as a function of  $E_i$  in Fig. 2(a). The intensity of the 2.1 eV feature is multiplied by 2 in order to show its resonance profile more clearly. Raw experimental data are plotted without any absorption corrections in this figure. For the 5.4 eV feature, the observed spectra were also fitted to a Lorentzian squared lineshape. The fitted intensity as a function of  $E_i$  (not shown) is virtually identical to the raw data shown in Fig. 2(a). However, the peak position of the 5.4 eV feature, plotted in Fig. 2(b), exhibits an interesting  $E_i$ -dependence. Specifically, there is a linear shift of the peak position from 5.4 eV at  $E_i = 8995$  eV to 5.6 eV at  $E_i = 9000$  eV; for  $E_i \gtrsim 9000$  eV, the peak position remains around 5.6 eV. An apparent peak position shift is also observed for  $E_i \lesssim 8995$  eV. However, the small intensity [shown in Fig. 2(a)] and the resultant large error bars for these data points make it difficult to analyze in quantitatively meaningful way. Thus, we will focus on the peak position shift for  $E_i \gtrsim 8995$  eV in what follows.

Such an apparent shift at first sight appears surprising. The natural expectation is that a valence excitation – such as this – would appear as a Raman-shift in a RIXS spectra, that is, a peak at a fixed energy-transfer, independent of the incident energy. However, in their RIXS study of  $\text{La}_2\text{CuO}_4$ , Abbamonte and coworkers also observed an incident energy dependence of the peak position.<sup>14</sup> They proposed an expression based on a shakeup picture in third order perturbation theory to explain the experimental results, following earlier theoretical work by Platzman and Isaacs.<sup>17</sup> Specifically, the scattered intensity  $w$  is expected to have the form

$$w = \frac{S_K(\mathbf{q}, \omega)}{[(E_i - E_K)^2 + \gamma_K^2][(E_f - E_K)^2 + \gamma_K^2]}, \quad (1)$$

where  $E_K$  and  $\gamma_K$  are adjustable parameters, and  $S_K$  describes an electronic excitation spectrum of interest. The key ingredient of Eq. (1) is that both incoming and outgoing resonances are included in the denominator. The shape of this function depends on the relative widths of

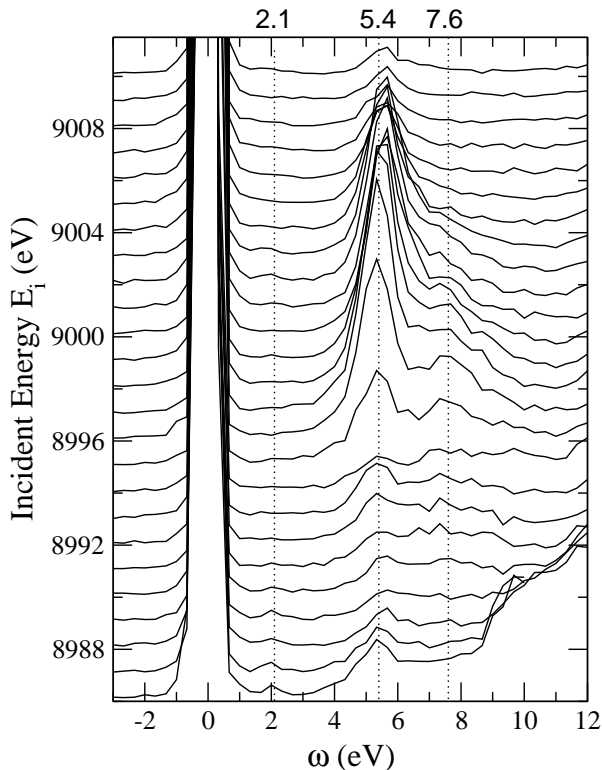


FIG. 1: Scattered intensity at  $\mathbf{Q}=(2.5\ 0.1\ 2.5)$  as a function of energy transfer,  $\omega$ . For clarity, scans are shifted vertically, and the incident energy for each scan can be read off from the vertical axis. The incident polarization was along the  $\mathbf{c}$ -direction (i.e., in the plane of the  $\text{CuO}_4$  plaquettes). Error bars are omitted for clarity.

the function  $S_K(\mathbf{q}, \omega)$  and the inverse lifetime,  $\gamma_K$ . For a sharp  $S_K(\mathbf{q}, \omega)$ ,  $\omega$  is peaked at constant energy transfer as a function of  $E_i$ . For a small value of  $\gamma_K$ , the peak exhibits characteristic dispersion. We have fitted all the data in the range of  $3 < \omega < 7$  from Fig. 1 to Eq. (1), using a Lorentzian squared function for  $S_K$  of full-width 1.1 eV. We have obtained a single set of parameters  $E_K \approx 8995$  eV and  $\gamma_K \approx 2.5$  eV. These parameter values are similar to those obtained in Ref. 14. By substituting the values of these parameters back in Eq. (1), we can reproduce the intensity and the peak position, which is plotted as a dashed line in Fig. 2. The fitting results indeed describe the observed peak shift and intensity on a *qualitative* level. However, it is not at all clear that this is a unique description of the data and further understanding of the discrepancy between the fit and the observed data will require a detailed model calculation as well as a microscopic theory of RIXS cross-section. We note that in the soft x-ray regime, there exist detailed model calculations to describe resonant emission spectroscopy experiments.<sup>18,19</sup>

Also shown in Fig. 2(b) is the measured x-ray absorption spectrum (solid line). The final states of this process are the intermediate states of the RIXS process. One can

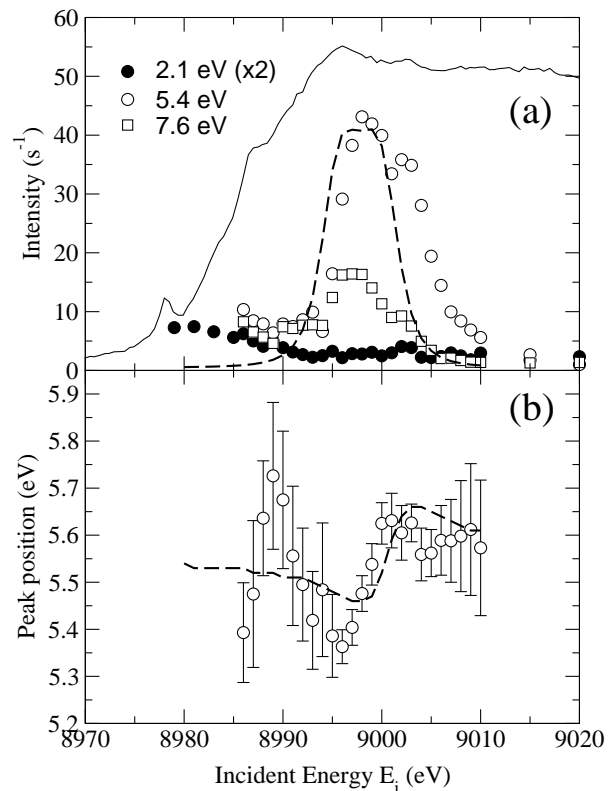


FIG. 2: (a) Scattered intensity at the three energy transfers, 2.1 eV, 5.4 eV, and 7.6 eV, as a function of  $E_i$  (raw data). Also plotted is the x-ray absorption, as measured by monitoring the fluorescence yield from the sample in the same scattering geometry (solid line). (b) The fitted peak position of the 5.4 eV feature as a function of  $E_i$ . The dashed lines in both figures are the results from fitting the data of Fig. 1 to Eq. (1), as described in the text.

associate the peaks around 8986 eV and 8996 eV in the absorption spectrum with the well-screened ( $\underline{1s}3d^{10}\underline{L}4p$ ) and poorly-screened ( $\underline{1s}3d^94p$ ) core hole final states, respectively, where  $\underline{1s}$  and  $\underline{L}$  denote holes in the core level and oxygen ligands, respectively. This association is consistent with the XAS studies on other insulating cuprates, including  $\text{CuGeO}_3$ .<sup>20</sup> We also observe a small pre-edge feature around  $E_i = 8978$  eV. Qualitatively similar results were obtained in the XAS study of  $\text{CuGeO}_3$  by Cruz et al.,<sup>20</sup> in which the pre-edge feature was assigned to electric dipole forbidden transitions from the Cu  $1s$  level to unoccupied Cu orbitals with  $3d$  character. The possible channels suggested for such transitions were (a) electric dipole transitions to Cu  $4p$  character mixed with neighboring Cu  $3d$  states, and (b) electric quadrupole transitions to the Cu  $3d$  states. In either case, the pre-edge feature, which is the intermediate state for the peak at 2.1 eV, has a strong  $3d$  character and will therefore have a large overlap with excitations involving  $3d$  electrons.

The intermediate states responsible for the resonant

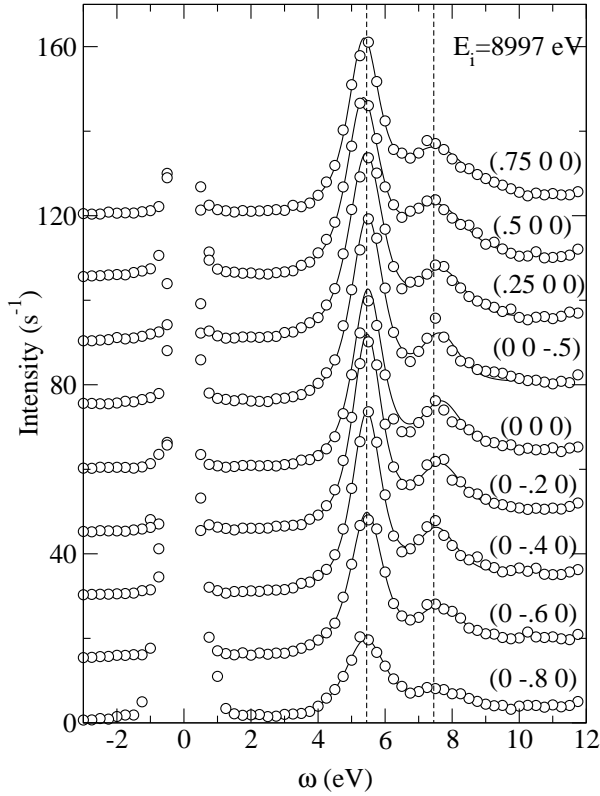


FIG. 3: Energy loss spectra taken at fixed  $E_i = 8997$  eV at a reduced wave vector [ $\mathbf{q} \equiv \mathbf{Q} - (203)$ ] as noted. Solid lines through the data points are the fit results as described in the text. Dashed lines show that the peak positions have very little  $\mathbf{q}$ -dependence. Each spectrum is offset vertically for clarity. Error bars are smaller than the symbol size.

enhancement of the high-energy features at 5.4 eV and 7.6 eV are the poorly-screened states. This is consistent with previous RIXS results obtained for quasi-2D cuprates  $\text{La}_2\text{CuO}_4$ <sup>16</sup> or  $\text{Nd}_2\text{CuO}_4$ .<sup>13</sup> However, the association of RIXS excitations with a particular intermediate states is not absolute. In Fig. 1, for example, the 5.4 eV feature seems to resonate at more than one intermediate state; that is, the intensity increases again as the incident energy decreases below  $\sim 8990$  eV. This needs further investigation.

### B. Momentum Dependence

To investigate the momentum dependence of these excitations, we have measured the energy-loss spectra along the high-symmetry directions [100], [010], and [001], around the (2 0 3) reciprocal lattice point. In Figs. 3 and 4, energy-loss scans taken with the incident energy fixed at  $E_i = 8997$  eV and  $E_i = 8987$  eV, respectively, are plotted at various momentum transfers. The reduced wave vector,  $\mathbf{q}$ , is noted for each scan. Vertical dashed lines are drawn to show the almost dispersionless behav-

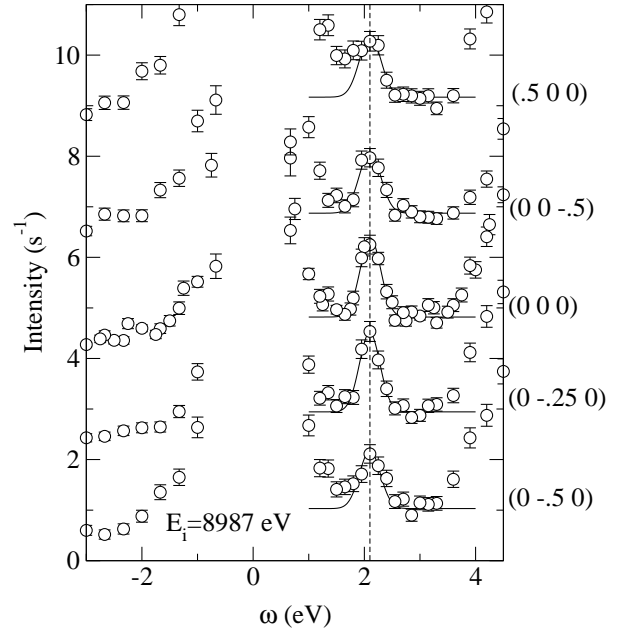


FIG. 4: Energy loss spectra for the 2.1 eV feature is shown with  $E_i = 8987$  eV for a fixed reduced wave vector ( $\mathbf{q}$ ) as noted. Solid lines through data points are fitting results as described in the text. Dashed lines show that the peak positions have very little  $\mathbf{q}$ -dependence. Each spectrum is offset vertically for clarity.

ior of the peaks at 5.4 eV and 7.6 eV in Fig. 3, and at 2.1 eV in Fig. 4. To obtain quantitative information on the dispersion of these excitations in Fig. 3, we fit the observed spectra with two peaks; both with a Lorentzian squared lineshape. We note here that these peaks are not resolution limited; the full-widths of the 5.4 eV peak and the 7.6 eV peak were fixed at 1.1 eV and 1.5 eV, respectively. The peak positions obtained from these fits are plotted in the upper two panels of Fig. 5. Due to its proximity to the much stronger peak at 5.4 eV, the location of the peak at 7.6 eV has rather large error bars, and more or less follows the dispersion of the 5.4 eV feature. As evident in Fig. 3, the energy dispersions of both excitations are very small along all high-symmetry directions. In particular, along the chain direction, [0 1 0], the 5.4 eV feature is virtually dispersionless. On the other hand, there is a suggestion of some dispersion ( $\sim 140$  meV) along the [1 0 0] direction, which is perpendicular to the copper-oxygen ribbon.

We attribute the 5.4 eV feature to a charge-transfer type excitation on a single copper-oxygen plaquette; specifically, we believe that it represents the energy difference between a bonding state and an antibonding state. Due to the strong hybridization between the Cu  $3d$  and O  $2p$  orbitals, the ground state for a half-filled copper-oxygen plane is not a simple  $3d^9$ . Rather, according to the Anderson impurity model,<sup>13</sup> it is a bonding state with an admixture of  $3d^9$  state and  $3d^{10}\bar{L}$  state. In the RIXS

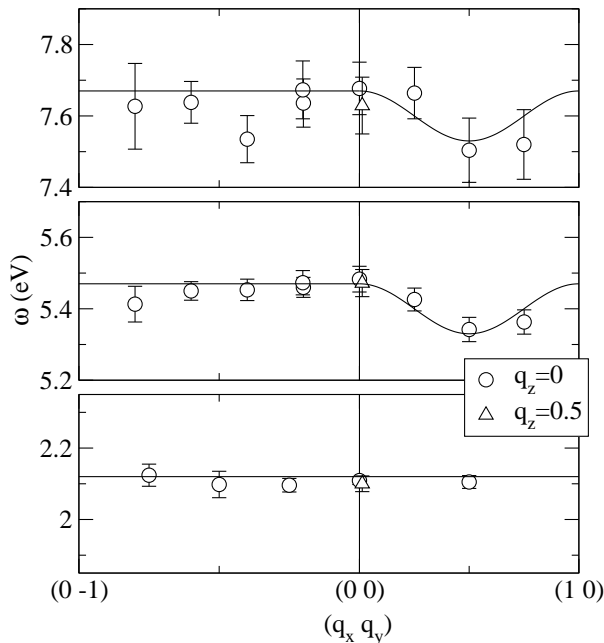


FIG. 5: The peak positions of the three features obtained from fitting scans shown in Figs. 2 and 3 to a Lorentzian-squared lineshape (5.4 eV and 7.6 eV) or a Gaussian lineshape (2.1 eV). Data on the left panels are taken at the position with  $\mathbf{q} \parallel (100)$ , and those on the right panels with  $\mathbf{q} \parallel (010)$ . The data taken at  $\mathbf{q}=(0\ 0\ -0.5)$  are shown as triangles.

process at the Cu K-edge, a Cu  $1s$  electron is excited to the Cu  $4p$  band, and this intermediate state may then decay into the antibonding excited state, producing the 6 eV feature commonly found in cuprate systems.<sup>13,14</sup> This interpretation is also consistent with the calculation by Weht and Pickett,<sup>8</sup> in which they found a splitting of  $\sim 5$  eV between the bonding and the antibonding states. Since this excitation is localized in a single plaquette of one copper and four oxygens, its excitation energy is somewhat material independent and would also be expected to have a very small momentum dependence. Recently, a small ( $\sim 150$  meV) dispersion along the chain direction has been observed for the 6.4 eV excitation of  $\text{CuGeO}_3$ .<sup>21</sup> Since this dispersion should depend critically on the angle  $\theta$  formed by Cu-O-Cu bond,<sup>4</sup> it is not surprising to observe smaller dispersion in  $\text{Li}_2\text{CuO}_2$  ( $\theta = 94^\circ$ ) than in  $\text{CuGeO}_3$  ( $\theta = 99^\circ$ ).

There are at least two possible interpretations for the 7.6 eV feature. First, the peak at 7.6 eV could arise from excitation of electrons from different bands than for the 5.4 eV feature. Alternatively, in the localized excitation picture described above, and in Ref. 7, one can have different excitation modes depending on the symmetry of the four oxygen orbitals in the plaquette. In this scenario, the 7.6 eV feature would involve the same bands, but differ from the 5.4 eV feature by the symmetry of the particle-hole pair. Further studies of polarization dependences might be able to distinguish between these two

possibilities.

We next discuss the momentum dependence of the 2.1 eV feature. In order to investigate this, the incident photon energy was held fixed at  $E_i=8987$  eV and energy loss scans were taken at a number of momentum transfers (Fig. 4). In contrast to the higher energy features, the 2.1 eV feature is found to be resolution limited at all momentum transfers and is therefore fitted to a single Gaussian lineshape. The peak position extracted in this way is plotted in the bottom panel of Fig. 5. It is clear that the energy dispersion of this peak is negligibly small. The two salient characteristics of the 2.1 eV feature are thus its lack of dispersion and its narrow peak width, which implies that this excitation is localized and has a long-lifetime. Another important point is that the intermediate states of this 2.1 eV feature are either  $3d$  states, or states having a large overlap with the  $3d$  states.

Based on these observations, we associate the 2.1 eV feature with a  $d-d$  type orbital excitation; that is, an excitation corresponding to exciting holes from the  $d_{yz}$  orbital to higher energy  $d$ -orbitals. According to the calculation of Tanaka et al.,<sup>22</sup> the energy splitting between the ground state,  $d_{yz}$ , and excited levels of  $d_{xy}$ ,  $d_{zx}$ ,  $d_{3x^2-r^2}$  in  $\text{Li}_2\text{CuO}_2$  is  $\sim 2$  eV, which is consistent with our value 2.1 eV. Similar  $d-d$  excitations have been observed in  $\text{CuGeO}_3$  with RIXS<sup>21</sup> and optical spectroscopies.<sup>23</sup>

#### IV. DISCUSSION

To summarize, we have observed energy loss features at 2.1 eV, which we attribute to a  $d-d$  excitation, and at 5.4 eV and 7.6 eV, which are attributed to localized charge-transfer excitations of copper oxygen plaquettes. These observations are generally consistent with the recent RIXS study of a similar edge-sharing chain compound  $\text{CuGeO}_3$ , with only a quantitative difference in the excitation energies. However, an additional excitation at 3.8 eV was observed for  $\text{CuGeO}_3$ . This was assigned to a non-local CT exciton mode formed by a particle and hole pair residing on neighboring plaquettes. The particle in this case forms a  $d^{10}$  state on one plaquette and the hole forms a Zhang-Rice (ZR) singlet state ( $d^9\bar{L}$ ) on the neighboring plaquettes.<sup>24</sup> The exciton state formed by this particle-hole pair can have a large dispersion of  $\sim 1$  eV in corner-sharing geometries such as  $\text{La}_2\text{CuO}_4$ ,<sup>16</sup>  $\text{Sr}_2\text{CuO}_3$ ,<sup>25</sup> or  $\text{SrCuO}_2$ .<sup>26</sup> In these cuprate materials (including  $\text{CuGeO}_3$ ), the RIXS peak corresponding to this CT exciton was observed at energies slightly higher than the CT gap energy as measured in optical conductivity [ $\sigma(\omega)$ ] studies. This trend is illustrated in Table I, where we list the RIXS peak positions and the corresponding optical conductivity peak positions in selected cuprate compounds. This difference presumably originates in the difference in the measured response functions. That is, the optical conductivity is proportional to the imaginary part of complex dielectric function,  $\text{Im}[\epsilon(\mathbf{q}=0, \omega)]$ , while the RIXS cross section is expected to follow the dielectric

TABLE I: RIXS peak position of CT exciton and corresponding peak position in optical conductivity  $\sigma(\omega)$ .

	RIXS (eV)	Ref.	$\sigma(\omega)$ (eV)	Ref.
CuGeO <sub>3</sub>	3.8	21	3.4	27
La <sub>2</sub> CuO <sub>4</sub>	2.2	16	2.0	28
SrCuO <sub>2</sub>	2.5	26	1.8	29

loss function,  $\text{Im}(-1/\epsilon(\mathbf{q}, \omega))$ .

In light of the above discussion, it seems clear that none of the observed features in Li<sub>2</sub>CuO<sub>2</sub> are such a non-local, exciton-like excitation. Consider first the case of the 2.1 eV feature, which we have previously argued as a  $d-d$  excitation. Were this excitation to be in fact, a non-local CT excitation, then, as discussed above, one would expect to observe a sharp feature in the optical conductivity just below this value, say around 1.9 eV. No such feature is observed in the optical data.<sup>4</sup> Rather, one observes a rapid increase of the optical conductivity above 2.6 eV which develops into peaks around 3.5 eV and 4.2 eV. In addition, as noted, the 2.1 eV feature is resolution limited, while CT exciton features are characterized by broad peaks in other materials.<sup>16,21,26</sup> Conversely, the feature at 5.4 eV is too high in energy to be associated with such a non-local excitation, both in terms of theoretical expectations for such an excitation and from the observed features in the optical conductivity data. Thus we conclude that such non-local CT exciton-like excitations are suppressed in Li<sub>2</sub>CuO<sub>2</sub>.

This immediately raises the question as to why such excitations are suppressed in this material. One possible explanation for this apparent absence lies in the different magnetic ground states of CuGeO<sub>3</sub> and Li<sub>2</sub>CuO<sub>2</sub>. This non-local CT exciton involves the movement of the hole on one copper site onto the oxygen orbitals of the neighboring plaquette where it forms a singlet state with the copper spin on that plaquette. This hole necessarily preserves the spin of the original Cu 3d hole. If neighboring copper spins are ferromagnetically coupled, as is the case for Li<sub>2</sub>CuO<sub>2</sub>, then a singlet state cannot be formed and only triplet excitations are possible. Since a significant fraction of the exciton formation energy comes from the binding energy of the Zhang-Rice singlet,<sup>30</sup> this excitation is likely to be significantly suppressed in such cases. Conversely, for the case of antiferromagnetic coupling of neighboring coppers, as in the case of CuGeO<sub>3</sub>, the singlet state may form naturally and the non-local excitation is stabilized. This argument was first made in the context of O K-edge RIXS spectra by Okada and Kotani<sup>31</sup> who showed just such an effect theoretically in calculated spectra for edge-sharing geometries, and it seems plausible that it is also active in the present

case. The absence of such an exciton would be consistent with the absence of a sharp feature near the CT gap in the optical conductivity data, and in fact, a recent theoretical calculation on a small cluster seems to support these ideas.<sup>32</sup> In any case, it is quite remarkable that the sign of the nearest-neighbor exchange coupling manifests itself at room temperature via the (non)existence of the RIXS peak from the CT exciton. This further emphasizes the delicate nature of bond angles and orbital overlap in determining the electronic properties of these strongly correlated cuprate systems.

Finally, in order to describe the apparent dispersion along the  $\mathbf{a}$ -direction, one needs to go beyond the simple picture of a localized excitation. As shown in Fig. 4, the features at 5.4 eV and 7.6 eV seem to exhibit non-zero dispersion along the  $\mathbf{a}$ -direction, with a minimum located at the zone boundary. This is similar to the dispersion behavior of the 6.4 eV excitation of CuGeO<sub>3</sub>,<sup>21</sup> although in that case dispersion was observed along the chain direction. If confirmed, this observation suggests that the interchain coupling along the  $\mathbf{a}$ -direction is not negligible. However, according to the calculation by de Graaf *et al.*<sup>12</sup>, the superexchange interaction via Li and O orbitals is too small to account for the non-zero dispersion behavior along this direction. A different exchange mechanism, such as direct exchange between Cu orbitals may need to be considered to understand this.<sup>6</sup>

In summary, we have observed three excitations in Li<sub>2</sub>CuO<sub>2</sub> using resonant inelastic x-ray scattering. These occur at 2.1, 5.4, and 7.6 eV and are attributed to a  $d-d$  excitation and two CT-type excitations, respectively. None of the excitations exhibit measurable dispersion along the chain direction consistent with the Cu-O-Cu bond angle being close to 90°. There is some evidence of dispersion perpendicular to the plane of the Cu-O ribbon for the CT-type excitations. This would suggest there is a non-zero interchain coupling. Finally, we find no evidence for a non-local (Zhang-Rice) CT exciton in the vicinity of the gap. We associate the suppression of such a feature with the ferromagnetic coupling between the neighboring copper spins.

### Acknowledgments

We would like to thank S. Maekawa and J. van den Brink for invaluable discussions. The work at Brookhaven was supported by the U. S. Department of Energy, Division of Materials Science, under contract No. DE-AC02-98CH10886. Use of the Advanced Photon Source was supported by the U. S. Department of Energy, Basic Energy Sciences, Office of Science, under Contract No. W-31-109-Eng-38.

<sup>1</sup> R. Hoppe and H. Riek, Z. Anorg. Allg. Chem. **379**, 157 (1970).

<sup>2</sup> F. Sapina, J. Rodriguez-Carvajal, M. J. Sanchis, R. Ibanes,

- A. Beltran, and D. Beltran, Solid State Commun. **74**, 779 (1990).
- <sup>3</sup> H. Ohta, N. Yamauchi, T. Nanba, M. Motokawa, S. Kawamata, and K. Okuda, **62**, 785 (1993).
  - <sup>4</sup> Y. Mizuno, T. Yohyama, S. Maekawa, T. Osafune, N. Motoyama, H. Eisaki, and S. Uchida, Phys. Rev. B **57**, 5326 (1998).
  - <sup>5</sup> M. Boehm, S. Coad, B. Roessli, A. Zheludev, M. Zolliker, P. Böni, D. McK Paul, H. Eisaki, N. Motoyama, and S. Uchida, Europhys. Lett. **43**, 77 (1998).
  - <sup>6</sup> R. Neudert, H. Rosner, S. L. Drechsler, M. Kielwein, M. Sing, Z. Hu, M. Knupfer, M. S. Golden, J. Fink, N. Nücker, M. Merz, S. Schuppler, N. Motoyama, H. Eisaki, S. Uchida, M. Domke, and G. Kaindl, Phys. Rev. B **60**, 13413 (1999).
  - <sup>7</sup> S. Atzkern, M. Knupfer, M. S. Golden, J. Fink, C. Waidacher, J. Richter, K. W. Becker, N. Motoyama, H. Eisaki, and S. Uchida, Phys. Rev. B **62**, 7845 (2000).
  - <sup>8</sup> R. Weht and W. E. Pickett, Phys. Rev. Lett. **81**, 2502 (1998).
  - <sup>9</sup> R. J. Ortega, P. J. Jensen, K. V. Rao, F. Sapina, D. Beltran, Z. Iqbal, J. C. Cooley, and J. L. Smith, J. Appl. Phys. **83**, 6542 (1998).
  - <sup>10</sup> U. Staub, B. Roessli, and A. Amato, Physica B **289-290**, 299 (2000).
  - <sup>11</sup> Y. Mizuno, T. Yohyama, and S. Maekawa, Phys. Rev. B **60**, 6230 (1999).
  - <sup>12</sup> C. de Graaf, I. de P. R. Moreira, F. Illas, O. Iglesias, and A. Labarta, Phys. Rev. B **66**, 014448 (2002).
  - <sup>13</sup> J. P. Hill, C. C. Kao, W. A. L. Caliebe, M. Matsubara, A. Kotani, J. L. Peng, and R. L. Greene, Phys. Rev. Lett. **80**, 4967 (1998).
  - <sup>14</sup> P. Abbamonte, C. A. Burns, E. D. Isaacs, P. M. Platzman, L. L. Miller, S. W. Cheong, and M. V. Klein, Phys. Rev. Lett. **83**, 860 (1999).
  - <sup>15</sup> M. Z. Hasan, E. D. Isaacs, Z. X. Shen, L. L. Miller, K. Tsutsui, T. Tohyama, and S. Maekawa, Science **288**, 1811 (2000).
  - <sup>16</sup> Y. J. Kim, J. P. Hill, C. A. Burns, S. Wakimoto, R. J. Birgeneau, D. Casa, T. Gog, and C. T. Venkataraman, Phys. Rev. Lett. **89**, 177003 (2002).
  - <sup>17</sup> P. M. Platzman and E. D. Isaacs, Phys. Rev. B **57**, 11107 (1998).
  - <sup>18</sup> H. Mizouchi, Phys. Rev. B **58**, 15557 (1998).
  - <sup>19</sup> K. Okada and A. Kotani, J. Phys. Soc. Japan **69**, 3100 (2000).
  - <sup>20</sup> D. Z. Cruz, M. Abbate, H. Tolentino, P. J. Schilling, E. Morikawa, A. Fujimori, and J. Akimitsu, Phys. Rev. B **59**, 12450 (1999).
  - <sup>21</sup> M. v. Zimmermann, J. P. Hill, C. C. Kao, T. Ruf, T. Gog, C. Venkataraman, I. Tsukada, and K. Uchinokura, unpublished (2001).
  - <sup>22</sup> N. Tanaka, M. Suzuki, and K. Motizuki, J. Phys. Soc. Japan **68**, 1684 (1999).
  - <sup>23</sup> M. Bassi, P. Camagni, R. Rolli, G. Samoggia, F. Parmigiani, G. Dhalenne, and A. Revcolevschi, Phys. Rev. B **54**, 11030 (1996).
  - <sup>24</sup> F. C. Zhang and T. M. Rice, Phys. Rev. B **37**, 3759 (1988).
  - <sup>25</sup> M. Z. Hasan, P. A. Montano, E. D. Isaacs, Z. X. Shen, H. Eisaki, S. K. Sinha, Z. Islam, N. Motoyama, and S. Uchida, Phys. Rev. Lett. **88**, 177403 (2002).
  - <sup>26</sup> Y. J. Kim, J. P. Hill, N. Motoyama, K. M. Kojima, S. Uchida, D. Casa, T. Gog, and C. T. Venkataraman, unpublished.
  - <sup>27</sup> A. Damascelli, D. van der Marel, G. Dhalenne, and A. Revcolevschi, Phys. Rev. B **61**, 12063 (2000).
  - <sup>28</sup> S. Uchida, T. Ido, H. Takagi, T. Arima, Y. Tokura, and S. Tajima, Phys. Rev. B **43**, 7942 (1991).
  - <sup>29</sup> Z. V. Popovic, V. A. Ivanov, M. J. Konstantinovic, A. Cantarero, J. Martinez-Pastor, D. Olgun, M. I. Alonso, M. Garriga, O. P. Khuong, A. Vietkin, and V. V. Moshchalkov, Phys. Rev. B **63**, 165105 (2001).
  - <sup>30</sup> F. C. Zhang and K. K. Ng, Phys. Rev. B **58**, 13520 (1998).
  - <sup>31</sup> K. Okada and A. Kotani, Phys. Rev. B **63**, 045103 (2001).
  - <sup>32</sup> S. Maekawa, private communications.